AL-Bahir
Journal for Engineering and Pure Sciences
BJEPS

Manuscript 1107

Beta Particles impact on the Optical Properties of TiO_2 thin films

Farah S. Dakhil

Hassan M.Jaber Al-Ta'ii

ORIGINAL STUDY

Beta Particles Impact on the Optical Properties of TiO_2 Thin Films

Farah S. Dakhil*, Hassan M.J. Al-Ta'ii

Department of Physics, College of Science, Al-Muthanna University, Iraq

Abstract

TiO_2 is a semiconductor with a wide band gap and is utilized in various applications, including photovoltaics, solar cells, and photocatalysis. In this work, TiO_2 thin films were fabricated using the doctor blade technique and deposited onto glass substrates. The purpose of the study was to investigate how beta irradiation affected the optical properties of the TiO_2 films. The produced samples' absorbance and photon energy were the main subjects of the measurements. While the samples exposed to beta rays for 30, 60, and 90 min had direct band gaps of 3.87 eV, 3.75 eV, and 3.66 eV, the sample that wasn't exposed to radiation had a direct energy band gap of 3.90 eV. After being exposed to radiation for 30, 60, and 90 min, the indirect band gap for the control sample dropped to 3.17 eV, 3.02 eV, and 3.28 eV from its initial value of 3.21 eV. These findings show that the direct and indirect energy band gaps gradually decrease as the duration of beta irradiation increases.

Keywords: Beta irradiation, TiO_2, Thin films, Band gap, XRD

1. Introduction

For over 150 years, researchers have shown significant interest in investigating thin films due to their diverse properties and wide range of applications when formed as thin layers [1]. These materials often require deposition on substrates such as glass or polymers due to their structural characteristics [2]. Titanium dioxide (TiO_2) thin films are widely used in optical devices thanks to their excellent optical properties and high chemical and thermal stability, even under harsh conditions [3]. They are employed in applications such as multilayer optical coatings (used as filters) [4], optical waveguides [5], and others. These films offer a high refractive index, strong transmittance in the visible light spectrum, and excellent durability. Furthermore, TiO_2 possesses an exceptionally high dielectric constant. Among its many advantageous features, TiO_2—being a well-known n-type semiconductor—exhibits high thermal stability, nontoxicity, a suitable band gap (approximately 3.2 eV for anatase and 3.0 eV for rutile), and excellent electron transport capability [6]. Because of these qualities, it is a great fit for a variety of applications, such as gas sensors, lithium-ion batteries, solar cells, photocatalysis, and photodegradation systems. [7,8]. In addition, its cost-effectiveness enhances its appeal for the development of efficient photoelectric devices [9]. The primary areas of application focus include use as electrode material, electron transport layers, and photosensitive materials [10−12]. In 2020, Mohammad Nurul Islam and colleagues, successfully created thin coatings of transparent and conductive titanium dioxide (TiO_2) by spray pyrolysis. Their research sought to use both theoretical and experimental methods to regulate the band gap of aluminum-doped TiO_2 films. When comparing aluminum-doped samples to undoped films, optical examination revealed a redshift in the absorption edge, suggesting that the metal inclusion had a

Received 6 June 2025; revised 5 August 2025; accepted 6 August 2025.
Available online 26 September 2025

* Corresponding author.
E-mail addresses: Sci.farah@mu.edu.iq (F.S. Dakhil), hassankirkukly@mu.edu.iq (H.M.J. Al-Ta'ii).

https://doi.org/10.55810/2313-0083.1107

smaller band gap. The theoretically expected shifts were closely matched by the optical band gap values, which ranged from 3.11 eV to 3.64 eV. In particular, the direct band gaps were between 3.70 eV and 3.49 eV, whereas the indirect band gaps were between 3.18 eV and 3.01 eV. These findings show how aluminum doping can effectively alter the optical characteristics of TiO_2 thin films, making them promising options for gas sensors and optoelectronic devices. [13]. In 2022, Tapash Chandra Paul et al., produced TiO_2 thin films with different Fe concentrations (0, 2, 4, 6, and 8 at.%), both undoped and Fe-doped. Utilizing a straightforward and economical spray pyrolysis method (SPT), the films were made using $Ti(OCH_2CH_2CH_2CH_3)_4$ as the precursor. According to the study, anatase to rutile phase transition was triggered by increasing Fe contents (4–8% at.%). Results from UV–Vis spectroscopy showed that the optical band gap decreased from 3.81 eV (0 % Fe) to 3.70 eV (8 % Fe), and absorption redshifted. [14]. In 2024, Kanmaz et al., investigated the effects of heat annealing on the optical characteristics of TiO_2 thin films produced using the sol–gel spin coating method on quartz glass substrates. The films were annealed for 1 h at temperatures ranging from 300 °C to 900 °C using a 0.5 M precursor solution. According to their research, the optical band gap decreased from 3.42 eV at 300 °C to 3.29 eV at 900 °C, indicating better crystallinity and increased visible light absorption as the annealing temperature rose. [15]. This study aims to understand the changes in the optical properties of TiO_2 thin films resulting from exposure to beta radiation, by analyzing the absorption coefficient and optical band gap, in order to clarify the relationship between radiation and the electronic structure of the material.

2. Experimental methodology

In this study, titanium dioxide "TiO_2" thin films were coated using a doctor blade onto glass substrates with dimensions of $1.1 \times 2\ cm^2$. After washing for 5 min in ethanol, they were rinsed for another 5 min in distilled water, and then rinsed for another 5 min in acetone to remove any contaminants. They were then dried in an oven at 50 °C for 15 min. A TiO_2 paste was prepared by mixing 3 g of TiO_2 powder with dilute nitric acid (5 ml) and a drop of ethylene glycol. Finally, after depositing the TiO_2 films on the glass, they were annealed for 30 min at 450 °C and then allowed to cool naturally, as shown in Fig. (1). The TiO_2 thin films were exposed to beta particles from the Sr-90 radioisotope source. UV–Vis spectroscopy was used to measure the samples. The Taue equation (1) was used to determine the optical band gap (Eg) [16]

For direct transitions equation (1)

$$(\alpha hv)^2 = A(hv - Eg) \tag{1}$$

For indirect transitions equation (2)

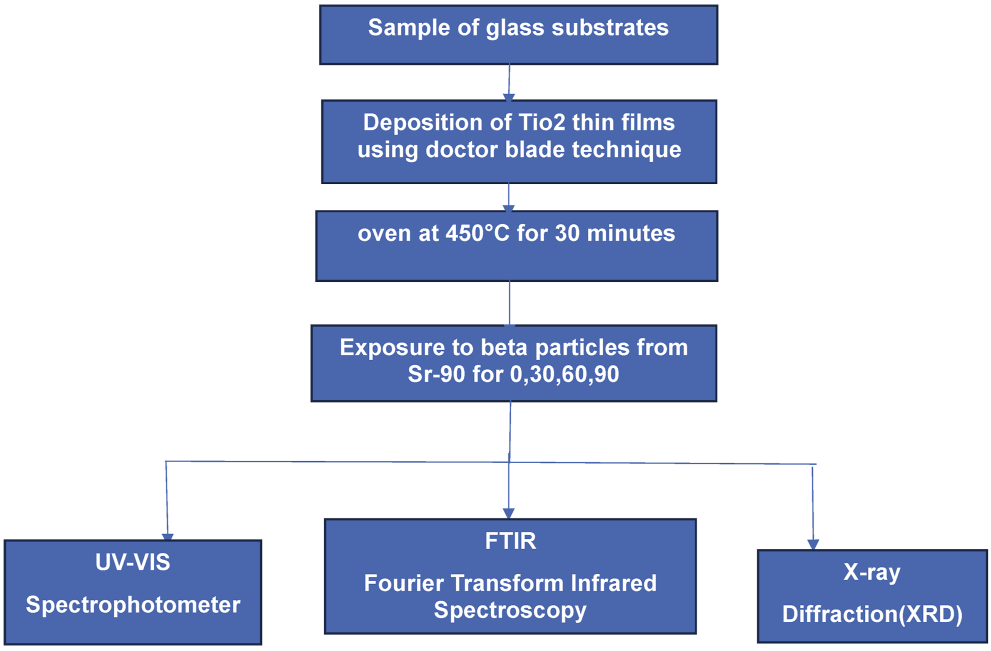

Fig. 1. Experimental work steps.

$$(\alpha hv)^{\frac{1}{2}} = B(hv - Eg) \quad (2)$$

Where A, B is a constant, The optical energy band gap is denoted by Eg, the photon energy by hv, the absorption coefficient by α, and the kind of transition by r.

The average crystallite size of TiO_2 films is calculated using Scherrer's formula and by XRD results through Eq (3) [17].

$$D = \frac{K\lambda}{\beta \cos\theta} \quad (3)$$

where λ is the x-ray wavelength (0.154 nm), β is the line broadening at FWHM in radians, θ is the Bragg's angle in degrees, K is the Scherrer constant (0.94) and D is the average crystallite size (nm) [18].

Bragg's law determines the interplanar distance or d-spacing values between the atoms in a crystal system by using Eq (4).

$$d = \frac{\lambda}{2 \sin\theta} \quad (4)$$

3. Results and discussion

The impact of beta radiation on titanium dioxide was investigated over different exposure times using beta particles emitted from a Sr-90 source. The UV–Vis spectroscopy results and optical characteristics of the samples are compared in Fig. (2), which displays the optical absorption spectra for irradiation durations of 0, 30, 60, and 90 min. Measurements were made between 300 and 800 nm in wavelength. Because of its low atomic density, pure TiO_2 has comparatively low absorption, as seen in Fig. (2), meaning that there are fewer atoms available to interact with input photons [19]. However, beta particle irradiation induces microstructural modifications in the TiO_2 thin films [20], leading to an increase in optical absorbance. This enhancement is attributed to charge trapping caused by radiolytic dissociation of molecules through radiation-generated electrons or holes [21], along with the creation of defect centers. The emission of electrons from the Sr-90 source contributes to hole trapping within the film's structure [22]. Fig. (2) also indicates that the absorption reaches its maximum after 90 min of exposure.

Fig. (3) shows how samples exposed to different amounts of beta irradiation relate to the photon energy and the direct optical band gap energy of TiO_2 thin films. Using Equation (1), the optical band gap of the non-irradiated TiO_2 layer was determined to be 3.90 eV. Following 30, 60, and 90 min of beta radiation exposure, the films' observed band gap values dropped to 3.87, 3.75, and 3.66 eV, respectively. This progressive decline suggests that the band gap narrows noticeably with increased beta dosages. Charge trapping, radiation-induced structural alterations, and defect state generation are all responsible for the decrease in band gap energy. In particular, the radiation-induced dissociation during the 90-min exposure creates defect centers and electron–hole pairs. The Sr-90 source's electrons help to trap holes in the structure of the film. Consequently, the optical band gap of the TiO_2 thin films visibly shrinks as a result of the buildup of these defects [23].

TiO_2 nanoparticles subjected to varying doses of beta radiation exhibited a noticeable decrease in

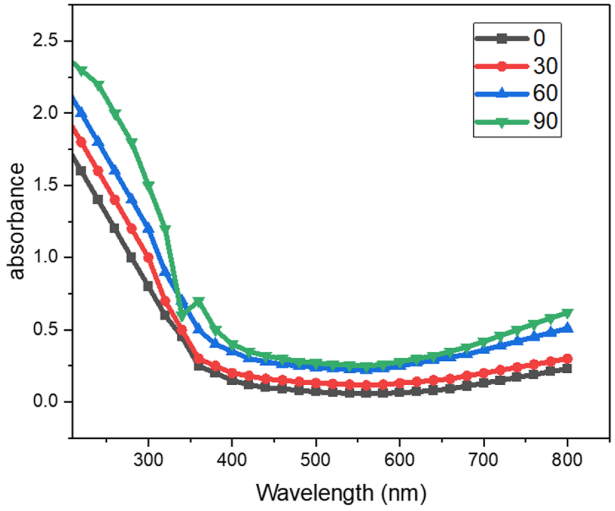

Fig. 2. The absorbance characteristics of samples for (0, 30,60, and 90) min.

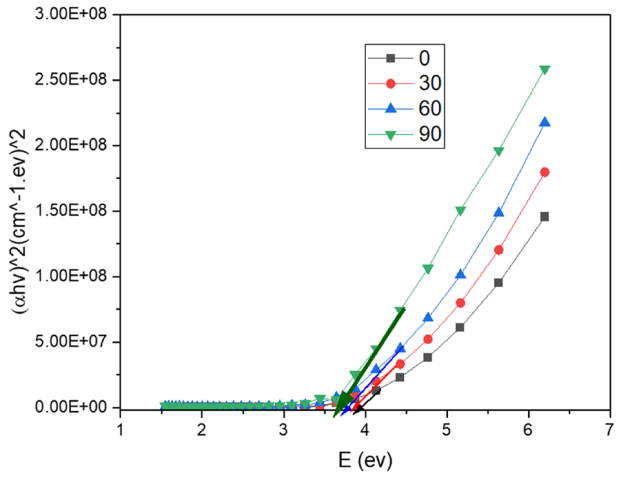

Fig. 3. The energy gap (hv) of the TiO_2 film for stander sample, 30 min, 60 min, 90 min.

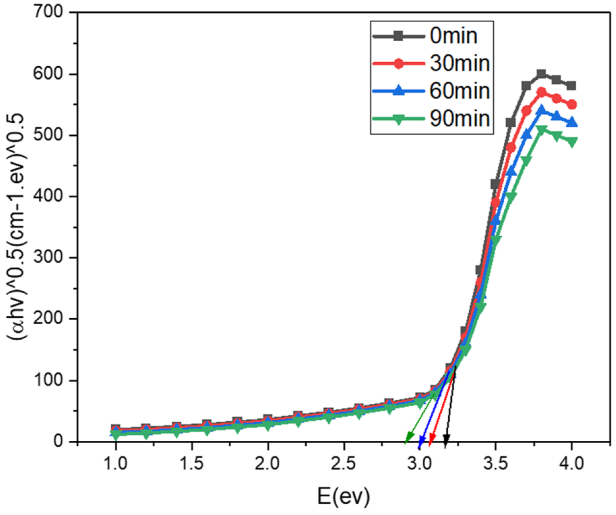

Fig. 4. Tauc plot (αhv) 0.5 corresponds to the. Energy gap (hv) of the TiO_2 film for stander.

optical band gap energy. As shown in Fig. 4, the unirradiated sample displayed a band gap of 3.21 eV. After exposure to beta radiation for 30, 60, and 90 min, the band gap values decreased to 3.17, 3.02, and 2.28 eV, respectively. These results clearly demonstrate that increasing the radiation dose leads to a gradual reduction in the optical band gap energy.

Table 1 shows that the energy band gap shrinks with increasing irradiation time. The TiO_2 is exposed when radiation breaks the Ti−O bonds to the vacancies and defects, which causes the defect to grow and the energy gap to shrink [24].

Fig. 5: demonstrates the temporal evolution of optical energy bandgaps under beta radiation exposure. The analysis reveals that both direct and indirect bandgap transitions exhibit maximum energy values at t = 0 min (pre-irradiation state), measuring 4.00 eV and 3.99 eV respectively. Subsequently, systematic degradation of the bandgap energies is observed as a function of beta radiation exposure time, with the direct transition showing more pronounced reduction rate compared to the indirect transition pathway.

Fourier-Transform Infrared (FTIR) Analysis. Fig. (6) presents the FTIR spectra of both irradiated

Table 1. Displays the energy gap for the direct and indirect irradiation times of TiO_2 films.

The duration of the irradiation sample	Gap in direct energy (eV)	Gap in indirect energy (eV)
0 min	3.90	3.21
30 min	3.87	3.17
60 min	3.75	3.02
90 min	3.66	2.28

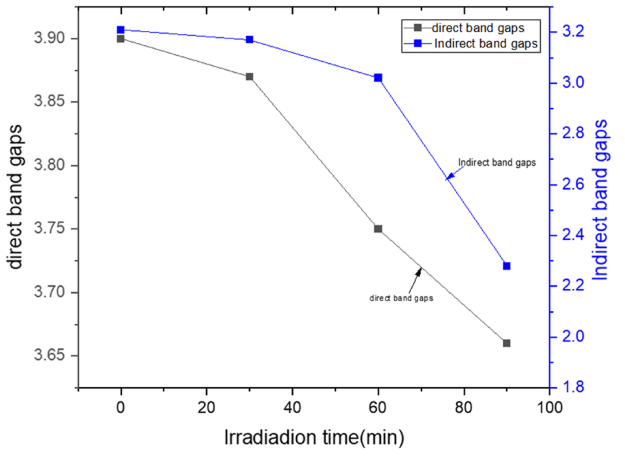

Fig. 5. Elucidate the direct and indirect band gaps in relation to exposure time.

and non-irradiated TiO_2 powder samples subjected to beta exposure for 30, 60, and 90 min. Three distinct absorption bands were observed. The most prominent band appeared at 3195 cm^{-1}, attributed to the stretching vibration of the hydroxyl (O−H) group. Another band was detected around 1517 cm^{-1} [25], which corresponds to the bending vibration of Ti−OH groups associated with adsorbed water. A notable Ti−O stretching mode was identified at 1055 cm^{-1}. Additionally, lattice vibrations of TiO_2 revealed bulk water absorption features at approximately 546 cm^{-1} [26] (see Table 2).

Fig. (7) X-ray diffraction (XRD) analysis was used to investigate the impact of beta radiation exposure at various time intervals (0, 30, 60, and 90 min) and reveal changes in the crystal structure of titanium dioxide (TiO_2). The observations, which include reduced crystallinity and alterations in the crystal

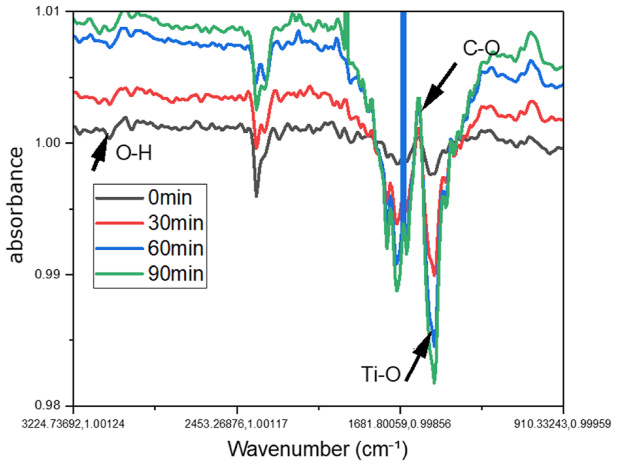

Fig. 6. FTIR spectra of TiO_2 film for different concentrations and irradiation times.

Table 2. The band type and wavenumber for each irradiation time.

Band Type	0 min	30 min	60 min	90 min
O–H Stretching	3224 cm^{-1}	3210 cm^{-1}	3203 cm^{-1}	3195 cm^{-1}
C–H Stretching	2453 cm^{-1}	2445 cm^{-1}	2438 cm^{-1}	2430 cm^{-1}
O–H Group bending	1681 cm^{-1}	1675 cm^{-1}	1670 cm^{-1}	1664 cm^{-1}
C=O C–O	1500 cm^{-1}	1511 cm^{-1}	1515 cm^{-1}	1517 cm^{-1}
C–N Stretching	1060 cm^{-1}	1066 cm^{-1}	1070 cm^{-1}	1073 cm^{-1}
Ti–O Stretching	910 cm^{-1}	904 cm^{-1}	899 cm^{-1}	896 cm^{-1}

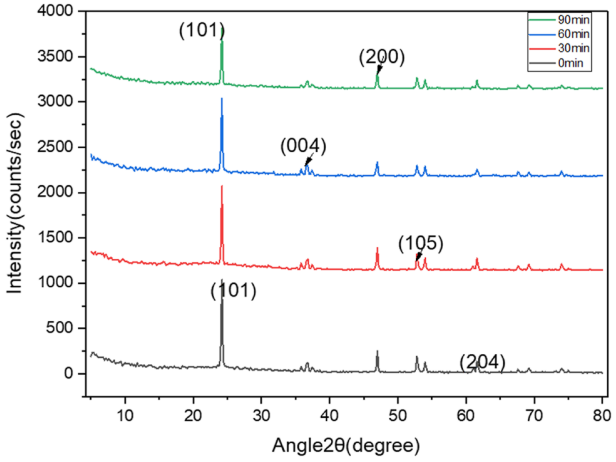

Fig. 7. XRD TiO_2 thin films.

lattice, confirm that beta irradiation affects the structural arrangement of the material at the atomic scale. The gradual decline in the intensity of certain diffraction peaks especially at 90 min may suggest a decrease in crystallinity or potential lattice damage, likely caused by the accumulation of defects and distortions induced by the energy of the beta particles [27].

The data in Table (3) Structure: A pure anatase TiO_2 phase is confirmed by X-ray diffraction (XRD) analysis, with significant peaks located at the (101), (004), (200), (105), and (204) planes. Radiation effect: Structural damage is shown by the intensity gradually decreasing with irradiation time. Preferential damage to this crystal plane is indicated by the (101) peak, which displays the largest drop (~20 %). Crystallinity: The anatase structure is preserved as the peak positions stay constant. Instead of total amorphization, point defect development is indicated by the intensity drop without peak broadening. Beta irradiation exhibits good radiation tolerance appropriate for nuclear applications by creating lattice defects in TiO_2 while maintaining the anatase structure. It is simpler to comprehend the main findings from XRD analysis because of this succinct approach, which offers the fundamental scientific information without going into great detail [28].

The data in Table (4) indicate that the crystallite size of TiO_2 decreased significantly after 90 min of beta irradiation compared to shorter periods. The size decreased to 26.76468 nm, indicating a negative effect of long-term irradiation on the crystalline structure of the material. This decrease can be

Table 4. Influence of beta irradiation duration on the crystallite and grain sizes of TiO_2 thin films as determined by XRD analysis using Scherrer's equation.

Samples	2θ (degree)	θ (degree)	FWHM (radian)	Crystallite size D (nm)	d (nm)
0min	24.2004	12.1002	0.2255	35.96391	0.36732
30min	24.2018	12.1009	0.2285	35.49164	0.36730
60min	24.207	12.1035	0.22952	35.33357	0.36722
90min	24.2112	12.1056	0.303	26.76468	0.36716

Table 3. XRD peak analysis of anatase TiO_2 under beta irradiation.

peak	2θ (degree)	hkl	Crystal System	Change with Time
1	25.3	(101)	Anatase	Decreasing intensity (radiation damage)
2	37.8	(004)	Anatase	Gradual decrease in intensity
3	48.0	(200)	Anatase	Moderate decrease over time
4	55.1	(105)	Anatase	Slight intensity reduction
5	62.7	(204)	Anatase	Minor decrease in crystallinity

explained by the physical effects and distortions resulting from high-energy irradiation. Beta irradiation generates crystalline defects (such as gaps and interatomic atoms) within the nanostructure of the material. With longer irradiation time, these defects and distortions accumulate further, reducing the crystalline order of the material and increasing internal stress. As a result, the average crystallite size as calculated by the Scherrer equation decreases as the peaks in the X-ray pattern widen (greater FWHM) [29].

4. Conclusion

Titanium dioxide (TiO_2) thin films synthesized using the doctor blade technique were investigated for their optical and structural properties under beta particle irradiation. UV−Vis spectroscopy showed that the unirradiated sample had a direct band gap of 3.90 eV and an indirect band gap of 3.21 eV. Upon exposure to beta irradiation for 30, 60, and 90 min, the direct band gap values decreased to 3.87, 3.75, and 3.66 eV, while the indirect band gaps were found to be 3.17, 3.02, and 2.28 eV, respectively. This gradual decrease in band gap energies indicates the emergence of localized states near the conduction band, resulting in an increased absorption coefficient with decreasing photon energy. FTIR analysis showed clear scattering within the wavenumber region (800−1000 μm), indicating internal structural changes in the films. Furthermore, X-ray diffraction (XRD) analysis revealed a slight shift in the diffraction angle (2θ) from 24.2004° to 24.2112°, indicating no significant phase transition or change in crystal structure. However, an increase in the full width at half maximum at the highest point was recorded from 0.2255 to 0.303°, implying an increase in lattice distortion, a decrease in crystallinity, and a decrease in average crystal size. This indicates that beta radiation contributed to the inhibition of crystal growth, as the crystal size decreased with prolonged irradiation.

Source of Funding

No funding was received for this research.

Conflict of interest

The authors declare no conflicts of interest.

Ethical Approval

None.

Data availability statement

No additional data are available.

Author Contributions

Farah S. Dakhil: Conceptualization, Methodology, Investigation, Data Curation, Writing − Original Draft.

Hassan M. Jaber Al-Ta'ii: Supervision, Project Administration, Writing − Review & Editing.

Acknowledgments

The authors would like to express their sincere gratitude to Dr. Hassan M. Jaber Al-Ta'ii for his valuable guidance and support throughout this work.

References

[1] Berger LI. Semiconductor materials. CRC Press; 2020.
[2] Kazmerski LL. Electrical properties of polycrystalline semiconductor thin films. Polycrystal Amorphous Thin Films Divices 1980:59−134.
[3] Bange K, Ottermann C, Anderson O, Jeschkowski U, Laube M, Feile R. Investigations of TiO2 films deposited by different techniques. Thin Solid Films 1991;197(1−2):279−85.
[4] Mardare D, Baban C, Gavrila R, Modreanu M, Rusu G. On the structure, morphology and electrical conductivities of titanium oxide thin films. Surf Sci 2002;507:468−72.
[5] Pinto F, Wilson A, Moss B, Kafizas A. Systematic exploration of WO3/TiO2 heterojunction phase space for applications in photoelectrochemical water splitting. J Phys Chem C 2022; 126(2):871−84.
[6] Gatou M-A, Syrrakou A, Lagopati N, Pavlatou EA. Photocatalytic TiO2-based nanostructures as a promising material for diverse environmental applications: a review. Reactions 2024;5(1):135−94.
[7] á Fang H, áWang Q, áWang H, et al. Adv Funct Mater 2019; 29:1809013.
[8] Wang Z, Wang H, Liu B, Qiu W, Zhang J, Ran S, et al. Transferable and flexible nanorod-assembled TiO2 cloths for dye-sensitized solar cells, photodetectors, and photocatalysts. ACS Nano 2011;5(10):8412−9.
[9] Meng A, Zhang L, Cheng B, Yu J. Dual cocatalysts in TiO2 photocatalysis. Adv Mater 2019;31(30):1807660.
[10] Ferhati H, Djeffal F, Martin N. Highly improved responsivity of self-powered UV−Visible photodetector based on TiO2/Ag/TiO2 multilayer deposited by GLAD technique: effects of oriented columns and nano-sculptured surface. Appl Surf Sci 2020;529:147069.
[11] Deng Y, Li S, Li X, Wang R. HI-assisted fabrication of Sn-doping TiO2 electron transfer layer for air-processed perovskite solar cells with high efficiency and stability. Sol Energy Mater Sol Cell 2020;215:110594.
[12] Yu Z, Liu H, Zhu M, Li Y, Li W. Interfacial charge transport in 1D TiO2 based photoelectrodes for photoelectrochemical water splitting. Small 2021;17(9):1903378.
[13] Islam MN, Podder J, Hossain KS, Sagadevan S. Band gap tuning of p-type al-doped TiO2 thin films for gas sensing applications. Thin Solid Films 2020;714:138382.
[14] Paul TC, Podder J, Paik L. Effect of Fe doping on the microstructure, optical and dispersion energy characteristics of TiO2 thin films prepared via spray pyrolysis technique. Results in Optics 2022;8:100235.
[15] Kanmaz İ, Tomakin M, Aytemiz G, Manõr M, Nevruzoğlu V. Influence of thermal annealing on the band-gap of TiO2 thin films produced by the sol-gel method. Recep Tayyip

Erdoğan Üniversitesi Fen ve Mühendislik Bilimleri Dergisi 2024;5(1):49–56.
[16] Aldhuhaibat MJ, Hussein M, Hyder M, Amana MS. Study of the irradiation effect by α-particles on optical properties of ZnO: 6% in thin films. In: Journal of Physics, 1484. IOP Publishing; 2020. p. 012003. 1.
[17] Paufler P, Barrett CS, Massalski TB. Structure of metals. New York, Toronto, Sydney, Paris Frankfurt/M: Pergamon Press Oxford; 1980. p. 654. Seiten, 113 Abbildungen, 19 Tabellen und über 1400 Literaturhinweise. Preis US $20.–," ed: Wiley Online Library, 1981.
[18] Zhang L, Jiang Y, Ding Y, Daskalakis N, Jeuken L, Povey M, et al. Mechanistic investigation into antibacterial behaviour of suspensions of ZnO nanoparticles against E. coli. J Nanoparticle Res 2010;12:1625–36.
[19] Ali I, Imanova G, Agayev T, Aliyev A, Bentalib A, Kurniawan TA, Mbianda XY, et al. Sustainable hydrogen production by water decomposition in gamma radiolysis with post-modification studies of nano-BeO photocatalyst. J Chem Technol Biotechnol 2025;100(7):1463–71. https://doi.org/10.1002/jctb.7876.
[20] Verma R, Kumar V, Kango S, Khilla A, Gupta R. Microstructural, wettability, and corrosion behaviour of TiO2 thin film sputtered on aluminium. J Cent S Univ 2024;31(7):2210–24.
[21] Tusseyev T, Kuykabayeva A, Danlybaeva A, Zulbuharova E, Doszhanov O. The effect of γ-ray-radiation on surface physicochemical processes on Al2O3. In: Journal of Physics: Conference Series. 2984. IOP Publishing; 2025. p. 012021. 1.
[22] Hussain J. Development of a telescope detector for Sr-90 detection. 2022.
[23] Kim BH, Kwon JW. Plasmon-assisted radiolytic energy conversion in aqueous solutions. Sci Rep 2014;4(1):5249.
[24] Bourezgui A, Kacem I, Daoudi M, Al-Hossainy AF. Influence of gamma-irradiation on structural, optical and photocatalytic performance of TiO 2 nanoparticles under controlled atmospheres. J Electron Mater 2020;49:1904–21.
[25] Abazović ND, Čomor MI, Dramićanin MD, Jovanović DJ, Ahrenkiel SP, Nedeljković JM. Photoluminescence of anatase and rutile TiO2 particles. J Phys Chem B 2006;110(50):25366–70.
[26] Al-Hossainy A, Ibrahim A. Facile synthesis, X ray single crystal and optical characterizations of Cu-diphenylphosphino-methane organic crystalline semi-conductors. J Optoelectron Adv Mater 2014;16:1472–80.
[27] Glusker JP, Trueblood KN. Crystal structure analysis: a primer. Oxford University Press; 2010.
[28] Thamaphat K, Limsuwan P, Ngotawornchai B. Phase characterization of TiO2 powder by XRD and TEM. Agriculture and Natural Resources 2008;42(5):357–61.
[29] Monshi A, Foroughi MR, Monshi MR. Modified Scherrer equation to estimate more accurately nano-crystallite size using XRD. World J Nano Sci Eng 2012;2(3):154–60.